COMMUNICATION

Linker permethylation as a means to foster valence tautomerism and thwart dimerization in ferrocenyl-triarylmethylium cations†

Moritz Nau,[a] Larissa A. Casper,[a] Gernot Haug,[a] Michael Linseis,[a] Serhiy Demeshko[b] and Rainer F. Winter [ID] *[a]

Permethylation of the phenylene linker in a cationic ferrocenyl-phenylthioxanthylium dyad increases the amount of the diradical ferrocenium thioxanthyl radical valence tautomer and aids in supressing dimerization of the latter and of the one-electron reduced neutral radical.

Valence tautomerism (redox isomerism) denotes a situation, where compounds with chemically different, redox-active constituents exist as two or more equilibrating isomers. These isomers differ with respect to their electron and spin density distributions, and hence the oxidation state assignments, and interconvert through an intramolecular electron transfer. The ensuing electronic bistability provides interesting perspectives for their use as stimuli responsive materials, for spintronics or, if the spin states and magnetic moments of the redox isomers differ, as molecule-based magnetic switches.[1–12]
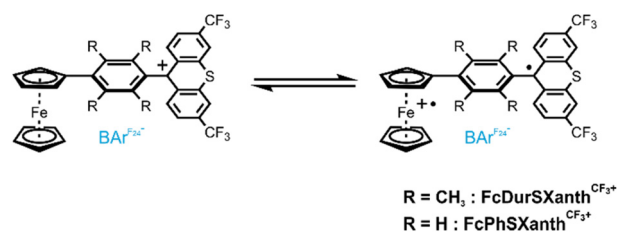
In 2003, Ratera, Veciana *et al.*, first reported on valence tautomerism in ferrocene-polychlorotriphenylmethyl (PTM) donor–acceptor dyads, where neutral ferrocene-PTM radical, Fc-PTM[•], and zwitterionic ferrocenium-polychlorotriphenyl-methanide, Fc[•+]-PTM[−], forms coexist in a thermal equilibrium.[13–15] Of more recent vintage is the demonstration of the same kind of isomerism in cationic ferrocene-triaryl-methylium dyads Fc-TAM[+].[16–18] At odds with Veciana's systems, the individual valence tautomers (VTs) here differ with respect to the number of unpaired spins, none for the Fc-TAM[+] ground state isomer, two for the higher energy ferrocenium-triarylmethyl form Fc[•+]-TAM[•]. As established by quantitative spin counting methods, the content of the diradical VT amounts to 6.3(±1.4)% for the ferrocene-9-phenylthioxanthy-lium dyad **FcPhSXanth**[CF3+] (Scheme 1, R = H),[19] rendering it a promising magnetochemical switch. Unfortunately, Fc[•+]-TAM[•] diradicals engage in monomer-dimer equilibria with formation of a covalent C–C bond between the methyl carbon atoms. This partially eliminates the organic spin, while leaving that on the ferrocenium constituents.

Further forays into this topic must therefore seek to shift the Fc-TAM[+] ⇌ Fc[•+]-TAM[•] equilibrium further to the side of the paramagnetic VT and, at the same time, suppress its dimerization. We felt that permethylation of the phenylene linker would serve both purposes by attenuating electronic coupling between the two redox sites owing to a larger torsion at the C–C linkages as well as counteracting dimerization due to increased steric bulk at the methyl C atom.

We therefore devised the duryl analog **FcDurSXanth**[CF3+] (Scheme 1, R = Me). It was synthesized in three steps starting from ferrocene boronic acid and *para*-dibromodurene, lithiation of the resulting bromodurylferrocene and subsequent attack of the carbon nucleophile to the keto function of the CF$_3$-substituted thioxanthone. The resulting carbinol **FcDurSXanth**[CF3]-**OH** was then converted into the target donor–acceptor dyad with the action of Brookhart's acid,[20] according to an established protocol.[18,19,21] Further details are provided in the ESI.†

FcDurSXanth[CF3]-**OH** was characterized by NMR spectroscopy and mass spectrometry (see Fig. S1–S4 of the ESI†). Of note is the broadening of specifically the methyl resonances

[a]*Fachbereich Chemie, Universität Konstanz, Universitätsstraße 10, 78457 Konstanz, Germany. E-mail: rainer.winter@uni-konstanz.de*
[b]*Institut für Anorganische Chemie, Georg-August-Universität Göttingen, Tammanstraße 4, 37077 Göttingen, Germany*

Scheme 1 . Cationic 4-ferrocenylphenylthioxanthylium complexes as the tetrakis[3,5-bis(trifluoromethyl)phenyl]borate (BAr$^{F24−}$) salts.

R = CH$_3$: **FcDurSXanth**[CF3+]
R = H : **FcPhSXanth**[CF3+]

at the duryl linker as a consequence of hindered rotation around the aryl–Cp and aryl–aryl bonds. These resonances sharpen to different degrees on warming. DFT-estimated activation energies are 43 and 144 kJ mol^{-1}.

^{1}H NMR resonances of the complex cation **FcDurSXanth^{CF3+}** are suspiciously broad, while those of the BAr^{F24-} anions remain sharp (Fig. S5 of the ESI†). This observation already points to the presence of also the paramagnetic ferrocenium-thioxanthyl diradical VT. Further characterization was achieved by mass spectrometry (Fig. S4 of the ESI†), combustion analysis and UV/Vis/NIR spectroscopy. Fig. 1 compares the electronic spectra of **FcDurSXanth^{CF3+}** and its non-methylated counterpart **FcPhSXanth^{CF3+}**.[18] TD-DFT-based band assignments are provided as Fig. S6 and S7 of the ESI.† A notable difference is the decreased oscillator strength and red shift of the so-called y_M band, which pertains to intramolecular charge transfer (CT) from the Fe^{2+} d$_\delta$ HOMO to the thioxanthylium-based LUMO. In contrast, the energy of the CT excitation from the π-orbitals of the cyclopentadienyl ligands to the same acceptor orbital (the so-called y-band)[22] experiences a sizable blue-shift of 3700 cm^{-1} (from 601 to 491 nm). Both are tokens of decreased electronic coupling between the donor and the acceptor moieties resulting from a large torsion between the Cp and the phenylene as well as the phenylene and the thioxanthylium ring planes. Of further note is the presence of a band at 643 nm (ε = 400 M^{-1}cm^{-1}), which our calculations assign to a thioxanthyl-to-ferrocenium CT excitation of the open shell diradical isomer (see Fig. S7 of the ESI†).

The electrochemical properties of **FcDurSXanth^{CF3+}** and its carbinol precursor were examined by cyclic voltammetry. The results are shown in Fig. 2 and in Fig. S8 and S9 of the ESI;† pertinent data are provided in Table 1 and Table S1† of the ESI.† CVs of **FcDurSXanth^{CF3+}** feature a reversible one-electron oxidation of the ferrocenyl entity at $E_{1/2}$ = 205 mV $vs.$ the FcH/FcH$^+$ reference couple as well as a reversible reduction of the cationic tritylium center at $E_{1/2}$ = 5 mV. The one-electron character of both redox processes was confirmed by chronoamperometry. At odds with all previous ferrocene-triarylmethylium dyads, **FcDurSXanth^{CF3+}** exhibits an additional, partially reversible second reduction to the corresponding carbanion at −1345 mV (Fig. S9 of the ESI†). This already hints at a com-
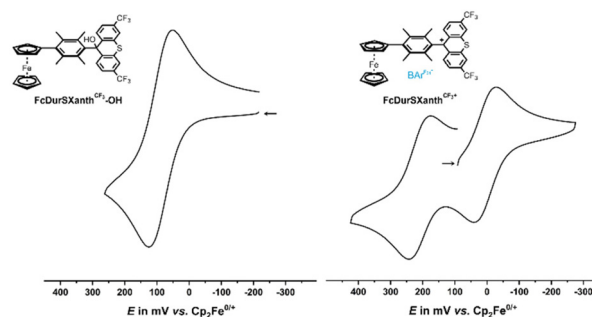
Fig. 2 Cyclic voltammogram of the carbinol precursor **FcDurSXanth^{CF3}-OH** and cationic complex **FcDurSXanth^{CF3+}** in CH$_2$Cl$_2$/NBu$_4^+$[BAr^{F24-}] (0.1 mM) at T = 293 K ($\pm$3 K) and at a scan rate v of 100 mVs^{-1}. The scan was initiated from the open-circuit potential.

**Table 1** Electrochemical data for phenylene-bridged ferrocene-thioxanthylium dyads and their carbinol precursors[a]

	$E_{1/2}^{+/2+}$ [mV]	$E_{1/2}^{+/U}$ [mV]	$\Delta E_{1/2}$ [mV]	$\Delta E^{H-L\,b}$ [eV][b]
FcDurSXanth^{CF3+}	205	5	200	1.54
FcPhSXanth^{CF3+}	295	0	295	1.78
FcDurSXanth^{CF3}-OH	85	n. a.	n. a.	−−
FcPhSXanth^{CF3}-OH	135	n. a.	n. a.	−−

[a] Potentials ($\pm$5 mV) in mV in CH$_2$Cl$_2$/NBu$_4^+$[BAr^{F24}]$^-$ (0.1 M) at T = 293 ($\pm$3) K and a scan rate v of 100 mVs^{-1} $vs.$ FcH/FcH$^+$. [b] DFT-calculated HOMO–LUMO gap.

paratively small degree of dimerization of the neutral radical form when compared to **FcPhSXanth^{CF3+}**[18] or other complexes of this type, at least on the voltammetric timescale. Comparison with non-methylated **FcPhSXanth^{CF3+}** reveals that permethylation of the phenylene linker decreases the half-wave potential for ferrocene oxidation by 90 mV, but has only a minute effect on thioxanthylium reduction. As a consequence, the half-wave potential separation $\Delta E_{1/2}$ is lowered from 295 to 200 mV. This is the smallest $\Delta E_{1/2}$ value of all **Fc-TAM$^+$** dyads reported to date.[18,19] Consistent with the closing of the HOMO–LUMO gap observed in the electronic spectra, the small $\Delta E_{1/2}$ indicates that the **FcDurSXanth^{CF3+}** and the **Fc$^{\bullet+}$DurSXanth$^{CF3\bullet}$** VTs are closer in energy than in all other compounds of this type.

Repeated attempts to crystallize **FcDurSXanth^{CF3+}** BAr^{F24-} finally yielded a crop of red-brown single crystals which were suitable for X-ray crystallography. The structure of the complex cation is displayed in Fig. 3; for further graphic displays see Fig. S10 and S11 of the ESI.† The anion shows no peculiarities and will not be considered further. **FcDurSXanth^{CF3+}** crystallizes in the triclinic space group $P\bar{1}$. Table 2 summarizes selected metric data of the complex cation (for a full listing of bond lengths, bond angles and dihedral angles see Tables S3–S5 of the ESI†).

The sp^2-hybridized carbenium carbon atom C21 adopts a trigonal planar environment with bond angles C16–C21–C22, C22–C21–C35, and C35–C21–C16 of 117.3(3)°, 122.8(3)°, and 120.0(3)°. The angle sum of 360° is in line with the expec-
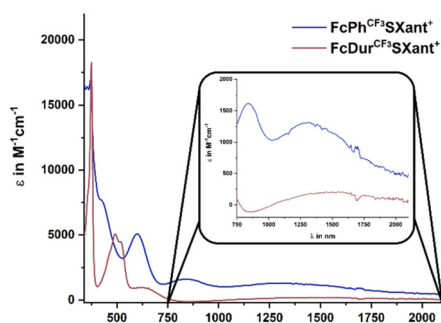
Fig. 1 UV/Vis/NIR absorption spectra of cationic complexes **FcDurSXanth^{CF3+}** and **FcPhSXanth^{CF3+}**.
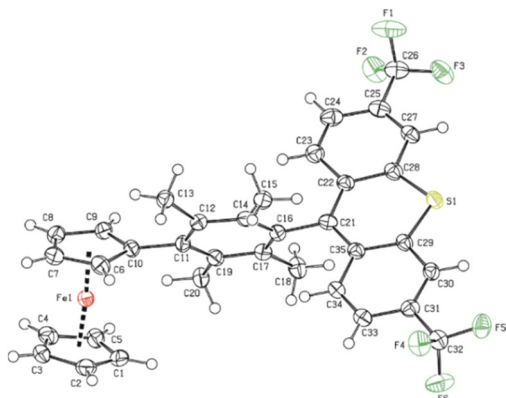
Fig. 3 ORTEP of the complex cation of **FcDurSXanth^{CF3+} BAr^{F24-}** salt. Thermal ellipsoids are displayed at the 50% probability level.

Table 2 Selected crystallographic data for **FcDurSXanth^{CF3+}** and their comparison with the geometry-optimized parameters for both isomers as obtained from DFT calculations[a]

	X-ray	DFT[b] diamagnetic	DFT[c] paramagnetic
$\sphericalangle_{Cp,Cp}$	6.61(18)°	5.87°	9.46°
$\sphericalangle_{Cp,Duryl}$	50.58(15)°	45.07°	44.40°
$\sphericalangle_{Duryl,Tx}$	77.69(12)°	84.87°	84.30°
d_{CpCp}	3.3032(4)	3.3110	3.3513

[a] All distances given in Å. [b] From DFT calculations with the PBE0 functional (charge: 1, multiplicity: 1). [c] From DFT calculations with the PBE0 functional (charge: 1, multiplicity: 3).

tations for a tritylium species and hence with the diamagnetic **FcDurSXanth^{CF3+}** VT. Steric repulsion between the *ortho* methyl substituents and the hydrogen atoms at C23 and C34 leads to a large torsion of 77.69(12)° between the thioxanthylium unit and the plane of durylene linker. This effect is attenuated for the linkage between the duryl and the sterically less demanding, five-membered Cp ring as indicated by the interplane angle of 50.58(15)°. This matches with the larger impact of phenylene permethylation on the half-wave potential of ferrocene oxidation as opposed to that of triarylmethylium reduction.

A further token of the diamagnetic VT in the crystalline state at the applied temperature of 100 K are relatively short distances between the Fe ion and the centroids of the Cp rings of 1.6536(4) and 1.6496(4) Å. These values match those of duryl-, 2,6-xylyl- or (pentaphenyl)phenyl substituted ferrocenes (range 1.641 to 1.659 Å) with similar tilt angles between the phenyl and Cp ring planes (range 41.90 to 51.06°),[23–25] and are appreciably smaller than those of *ca.* 1.70 Å in ferrocenium ions.[25–27] The tilt angle of 6.61(18)° between the Cp rings resembles those of 4.6 to 8.2° in the ferrocenes mentioned above and is thus likely due to steric pressure exerted by the methyl substituents, rather than indicating significant ferrocenium character. We also note the excellent match between the experimental Fe–Cp$_{centr.}$ distance and the computed value for the low-spin Fc-TAM$^+$ isomer as contrasting to the larger distance in the high-spin Fc$^{•+}$-TAM$^•$ form (Table 2).

Mössbauer spectra showed only a single doublet with an isomeric shift δ of 0.55/0.49 mm s^{-1} and a quadrupole splitting ΔE_Q of 2.38/2.380 mm s^{-1} at 80 and 250 K, respectively (see Fig. S12 of the ESI†). These values are typical for neutral ferrocene species.[16,19,28,29] EPR studies on single crystals nevertheless provided a weak EPR signal at $g = 2.0047$, which can be assigned to an organic spin centred at the (duryl)(thioxanthyl)methyl entity (see Fig. S13 of the ESI†). This points to the coexistence of a small fraction of the diradical VT under these conditions, which is however too small to be detected by Mößbauer spectroscopy.

Dissolved samples of the salt yield an EPR signal of much larger intensity at an identical g value as was observed in the solid state, however with much better resolved hyperfine couplings to nearby protons (Fig. 4; for the derived hfs values and a comparison between the experimental and the simulated spectra, see Table S6 and Fig. S14 of the ESI†). *T*-dependent measurements indicate that, contrary to the expectations based on the Boltzmann distribution between the ground and the excited state, the EPR signal intensity decreases over the temperature range of 20 °C to −100 °C, but then increases in the glassy state on further cooling to −150 °C. Such behaviour might originate from either an increasing population of the diradical VT on warming, enhanced dimerization of the diradical VT on lowering *T*, or both. Unfortunately, the expected Fe centred spin of the paramagnetic **Fc$^{•+}$DurSXanth$^{CF3•}$** VT was not observed even at 10 K (see the left panel of Fig. S12 of the ESI†).

In order to estimate the extent of dimerization of the **Fc$^{•+}$DurSXanth$^{CF3•}$** isomer, we studied its one-electron reduced form, the **FcDurSXanth$^{CF3•}$** radical, by quantitative EPR spin counting methods according to an established protocol.[18] **FcDurSXanth$^{CF3•}$** was prepared by *in situ* reduction of the cation with 1.1 equivalents of decamethylferrocene ($E_{1/2}{}^{0/+} = -590$ mV *vs.* FcH/FcH$^+$). Comparison of the double integral under the EPR curve with a calibration line obtained for variously concentrated solutions of the stable diphenylpicrylhy-
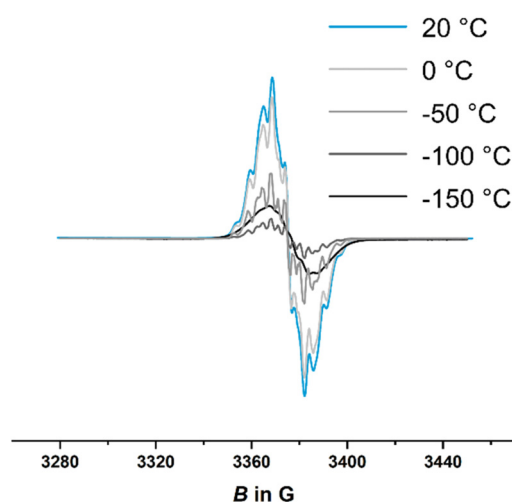
Fig. 4 *T*-dependent EPR spectra of **FcDurSXanth^{CF3+} BAr^{F24-}** in CH$_2$Cl$_2$.

drazyl radical dpph[.] as the standard yielded a free radical content of 92(±5)% (see Fig. S15 of the ESI†). This surpasses the value of 41(±6)% for **FcPhSXanth**$^{CF3\cdot 18}$ significantly. If one assumes that the neutral mono- and the cationic diradical VT dimerize to the same extent, which seems reasonable due to the large spatial separation between the Fe-localized charges in a hexaphenylethane-type dimer,[15,18] the doubly integrated EPR signal intensity of **FcDurSXanth**$^{CF3+}$ translates into a 10.0 (±1.4)% fraction of the diradical VT at 293 K. This surpasses the value of 6.3(±1.4)% for its non-methylated counterpart **FcPhSXanth**$^{CF3+}$ (for quantitative EPR spectroscopy and DFT-computed spin density distributions of **FcPhSXanth**$^{CF3\cdot}$ and **Fc**$^{\cdot +}$**PhSXanth**$^{CF3\cdot}$, see Fig. S16 and S17 of the ESI†). The increased content of the diradical VT in **FcDurSXanth**$^{CF3+}$ agrees with the lower half-wave potential separation between ferrocene oxidation and triarylmethylium reduction $\Delta E_{1/2}$ and hence a lower difference of the free enthalpies ΔG of the VTs.

In summary, we report that permethylation of the phenylene linker in a 4-ferrocenylphenyl-thioxanthylium dyad Fc-TAM$^+$ is an appropriate means to increase the amount of the diradical valence tautomer Fc$^{\cdot +}$-TAM$^{\cdot}$. Large ring torsions at the ferrocenyl-phenylene-thioxanthylium linkages, as verified by X-ray structure analysis, reduce electronic coupling between the donor and the acceptor. This in turn diminishes the energy offset between the diamagnetic and diradical VTs by closing the HOMO–LUMO gap. Furthermore, steric hindrance exerted by the methyl substituents on the durylene linker suppresses dimerization. As a result, the free radical content of the diradical VT increases from 6% to 10% at r. t. as verified by quantitative spin counting with only minor dimerization of the diradical VT. These findings thus provide a guideline for the purposeful design of donor–acceptor dyad-based magnetochemical switches.

Conflicts of interest

There are no conflicts to declare.

Acknowledgements

References

1 A. Dei, D. Gatteschi, C. Sangregorio and L. Sorace, *Acc. Chem. Res.*, 2004, **37**, 827–835.

2 C. G. Pierpont, *Coord. Chem. Rev.*, 2001, **217**, 99–125.

3 P. Gütlich, Y. Garcia and T. Woike, *Coord. Chem. Rev.*, 2001, **219–221**, 839–879.

4 A. Witt, F. W. Heinemann, S. Sproules and M. M. Khusniyarov, *Chem. – Eur. J.*, 2014, **20**, 11149–11162.

5 T. Tezgerevska, K. G. Alley and C. Boskovic, *Coord. Chem. Rev.*, 2014, **268**, 23–40.

6 N. A. Vázquez-Mera, F. Novio, C. Roscini, C. Bellacanzone, M. Guardingo, J. Hernando and D. Ruiz-Molina, *J. Mater. Chem. C*, 2016, **4**, 5879–5889.

7 A. Singh, S. Panda, S. Dey and G. K. Lahiri, *Angew. Chem., Int. Ed.*, 2021, **60**, 1–6.

8 Y.-Q. Li, J.-W. Dai, M. Wang, M. Yamashita and Z.-Y. Li, *Cryst. Growth Des.*, 2022, **22**, 4453–4462.

9 A. Dei and L. Sorace, *Appl. Magn. Reson.*, 2010, **38**, 139–153.

10 J. Dietrich, U. Thorenz, C. Förster and K. Heinze, *Inorg. Chem.*, 2013, **52**, 1248–1264.

11 E. Evangelio and D. Ruiz-Molina, *C. R. Chimie*, 2008, **11**, 1137–1154.

12 A. Rajput, A. K. Sharma, S. K. Barman, A. Saha and R. Mukherjee, *Coord. Chem. Rev.*, 2020, **414**, 213240.

13 I. Ratera, D. Ruiz-Molina, F. Renz, J. Ensling, K. Wurst, C. Rovira, P. Gütlich and J. Veciana, *J. Am. Chem. Soc.*, 2003, **125**, 1462–1463.

14 G. D'Avino, L. Grisanti, J. Guasch, I. Ratera, J. Veciana and A. Painelli, *J. Am. Chem. Soc.*, 2008, **130**, 12064–12072.

15 J. Guasch, L. Grisanti, S. Jung, D. Morales, G. D'Avino, M. Souto, X. Fontrodona, A. Painelli, F. Renz, I. Ratera and J. Veciana, *Chem. Mater.*, 2013, **25**, 808–814.

16 S. Oßwald, L. A. Casper, P. Anders, E. Schiebel, S. Demeshko and R. F. Winter, *Chem. – Eur. J.*, 2018, **24**, 12524–12538.

17 L. A. Casper, S. Oßwald, P. Anders, L.-C. Rosenbaum and R. F. Winter, *Z. Anorg. Allg. Chem.*, 2020, **81**, 3484–3499.

18 L. A. Casper, L. Wursthorn, M. Geppert, P. Roser, M. Linseis, M. Drescher and R. F. Winter, *Organometallics*, 2020, **39**, 3275–3289.

19 L. A. Casper, M. Linseis, S. Demeshko, M. Azarkh, M. Drescher and R. F. Winter, *Chem. – Eur. J.*, 2021, **27**, 10854–10868.

20 M. Brookhart, B. Grant and A. F. Volpe, *Organometallics*, 1992, **11**, 3920–3922.

21 L. A. Casper, V. Ebel, M. Linseis and R. F. Winter, *Dalton Trans.*, 2021, **50**, 15336–15351.

22 D. F. Duxbury, *Chem. Rev.*, 1993, **93**, 381–433.

23 S. Janková, I. Císarová, F. Uhlík, P. Stepnicka and M. Kotora, *Dalton Trans.*, 2009, 3137–3139.

24 J. E. Kim, S. U. Son, S. S. Lee and Y. K. Chung, *Inorg. Chim. Acta*, 1998, **281**, 229–234.

25 H. K. Gupta, S. Brydges and M. J. McGlinchey, *Organometallics*, 1999, **18**, 115–122.

26 X.-C. Wang, Y.-P. Tian, Y.-H. Kan, C.-Y. Zuo, J.-Y. Wu, B.-K. Jin, H.-P. Zhou, J.-X. Yang, S.-Y. Zhang, X.-T. Tao and M.-H. Jiang, *Dalton Trans.*, 2009, 4096–4103.

27 R. Martinez and A. Tiripicchio, *Acta Crystallogr. A*, 1990, **46**, 202–205.

28 G. Neshvad, R. Roberts and J. Silver, *J. Organomet. Chem.*, 1982, **236**, 237–244.

29 R. Roberts and J. Silver, *J. Organomet. Chem.*, 1984, **263**, 235–241.